https://doi.org/10.3311/PPee.14437

Periodica Polytechnica Electrical Engineering and Computer Science, 64(2), pp. 115–132, 2020

Power Quality and Capability Enhancement of a Wind-Solar-Battery Hybrid Power System

Belgacem Toual[1*], Lakhdar Mokrani[2], Abdellah Kouzou[1], Mohamed Machmoum[3]

[1] Applied Automation and Industrial Diagnostics Laboratory (LAADI), Faculty of Sciences and Technology, Ziane Achour University of Djelfa, P. O. B. 3117, Moudjbara Street, 17000 Djelfa, Algeria
[2] LACoSERE Laboratory, Department of Electrical Engineering, Faculty of Technology, University Amar Telidji of Laghouat, P. O. B. G37, Route de Ghardaia, 03000 Laghouat, Algeria
[3] IREENA, 37 Boulevard de l'Université, P. O. B. 406, 44602 Saint-Nazaire, Nantes, France
[*] Corresponding author, e-mail: toualb@gmail.com

Received: 24 May 2019, Accepted: 22 October 2019, Published online: 07 January 2020

Abstract

The Adrar site located in the south of Algeria, presents the most important windy and sunny site in Algeria that can be exploited. In this context for the exploitation of the two complimentary sources of this site (wind and sun) based on the meteorological data, the present paper focuses on the study of a Hybrid System (HS) based on an interconnection between a Wind Energy Conversion System (WECS) and a Photovoltaic System (PVS) which is planted in the DC-link bus of the back-to-back converter feeding the Double Feed Induction Generator (DFIG) rotor of the WECS. The objective of using this proposed coupling topology is to exploit the two available complementary renewable sources in the same time, to enhance the exploitation rate of the un-resized WECS back-to-back converter which remains at low power in the weak wind case or in the synchronism case and to eliminate the PVS inverter. Consequently the overall cost of the HS can be reduced. On the other side, to solve the energy quality problem; a modified MPPT mode control technique is proposed and compared with two other conventional techniques, the first one uses the PVS to offset only the WECS power rapid fluctuations and the second one uses a Battery Storage Unit (BSU) to ensure the produced energy smoothing. This BSU plays also an interesting role to store the surplus of energy when the maximum power level of the WECS converter is reached in case of wind and/or irradiation abundances.

Keywords

Algeria desert, Adrar site, hybrid power system, wind energy conversion system, photovoltaic system, battery storage unit, energy management, power quality enhancement

1 Introduction

Recently, the continued progress in many industrial and domestic sectors has resulted in a consistent rise in electricity demand. Annual Energy Outlook 2015 (AEO 2015) shows that the total electricity consumption grows with an average of 0.8 % per year, where the total consumption will pass from 3.836 billion kWh in 2013 to 4.797 billion kWh in 2040 [1].

The relatively slow rate of growth in demand, combined with the rising of natural gas prices, the environmental regulations, and the continuous growth in renewable generation, leads to tradeoffs among the fuels used for electricity generation.

From 2000 to 2012, the electricity generation based on natural gas-fired plants increased to more than double as the natural gas prices fell to relatively low levels. According to [1], the natural gas-fired generation will remain below 2012 levels until 2025, while the generation from existing coal-fired plants, the new nuclear and the renewable plants increases (see Fig. 1 (a)).

It can be noted from Fig. 1 (a) that the production of renewable energy begins to evolve from 9 % in 2000 to 18 % in 2040 of the global production. Therefore, renewable generation grows substantially from 2013 to 2040 in all types, especially for wind and solar generation

Cite this article as: Toual, B., Mokrani, L., Kouzou, A., Machmoum, M. "Power Quality and Capability Enhancement of a Wind-Solar-Battery Hybrid Power System", Periodica Polytechnica Electrical Engineering and Computer Science, 64(2), pp. 115–132, 2020. https://doi.org/10.3311/PPee.14437

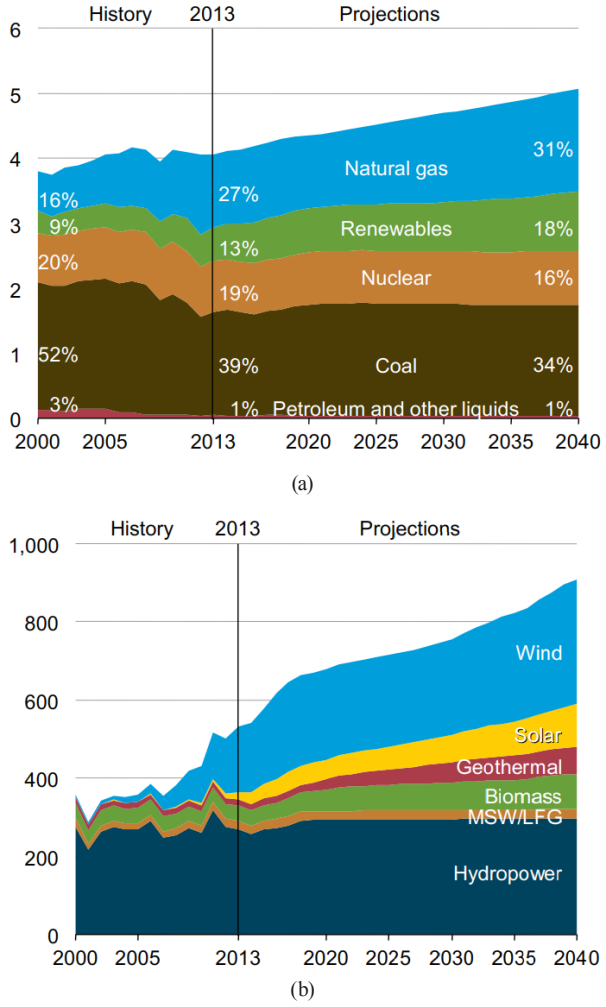

Fig. 1 (a) Assessment of the participation rate of different energy sources in the world electricity production, 2000-2040, (Trillion kWh) [1] (b) Assessment of the participation rate of renewable energy sources in the world electricity production, 2000-2040 (Billion kWh) [1]

(see Fig. 1 (b)). In 2013, as a result of the increases in wind and solar generation, the total non hydropower renewable generation was almost equal to hydroelectric generation for the first time. It will reach about two-thirds of the total renewable generation in 2040 [1].

Therefore, it can be seen that, WEC and PV systems are becoming important parts of the electrical power generation. Their basic energy sources (wind and solar) present the right choice due to the world abundance of windy sites and illuminated sites as well as windy and illuminated sites all over the globe. In addition, these sources are clean, economic, sustainable, safe, not expensive and easy to operate, especially for the photovoltaic systems, where there is no noise, not a lot of maintenance and no additional mechanical requirement [2, 3].

For this reason, the researches in the wind and photovoltaic hybrid power systems field are actually attracting more attention, especially concerning their internal conception, their hybridization, their coupling with the grid and their equipment by electrical energy storage tools to compensate their fluctuation and stochasticity.

Nowadays, in the wind farms, different WECS topologies are used according to the type of the used generator (synchronous, permanent magnet synchronous, with variable reluctance, or doubly-fed asynchronous, ...), its coupling method with the network (through power converters between network and stator or between rotor and network), and the method of its coupling with other renewable and storage sources.

Indeed, variable-speed wind turbines are currently the most used wind energy conversion system. The Doubly-Fed-Induction Generator (DFIG) based wind energy conversion system, also is known as an improved variable-speed WECS. So, it (DFIG) is presently the most popular generator which is used for the wind energy application [4, 5].

Various control schemes have been developed to enhance the performance of wind-source DFIG systems, including management of their power production, with other sources such as PVS and Permanent Magnet Synchronous Generator (PMSG) [6-8].

In order to minimize the inverters number and size, a special topology where the DFIG is connected to the network via its stator and controlled via its rotor has been used [6-8]. Its DC bus receives an addition DC power, from the photovoltaic and battery sources via their DC/DC converters. This topology has several advantages, such as the use of small rotor inverters (a third of DFIG power), reduced harmonics content, maximum exploitation of the back-to-back inverter especially in DFIG synchronous regime (no rotor power), and prevent the inverters availability without function at night (case of inverter between grid and systems based solely on the PV source).

Some hybrid configurations based on the DFIG have been used in practice (see Fig. 2) [4, 6-8]. Ghoddami et al. [7] (Fig. 2 (a)), have studied a Wind-PV-Battery hybrid system, where the PVS has been interfaced with the storage battery presenting the DFIG DC bus through its individual converter. Despite its lower number of power electronic converters, this system has not allowed the good control of the power and the SOC of batteries to ensure their insulation in fully charged case.

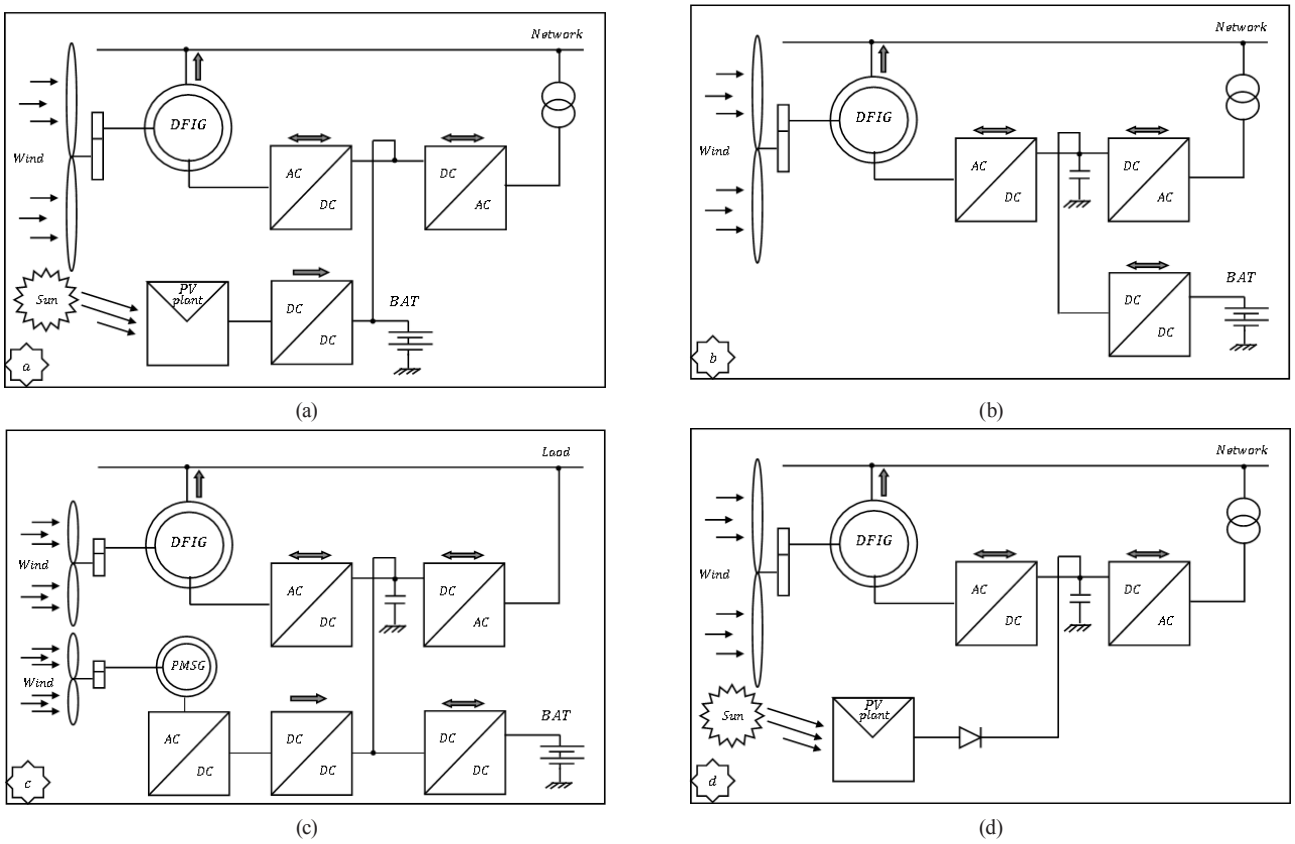

Fig. 2 (a) DFIG WECS coupled with PVS and BSU without converter (b) DFIG WECS coupled with BSU (c) DFIG WECS coupled with PMSG WECS and BSU (d) DFIG WECS coupled with PV plant without converter

Kahla et al. [4], Mendis and Muttaqi [8] (Fig. 2 (b), (c) respectively), have proposed other renewable power systems focussing on the battery power management with a DC buck-boost bidirectional converter. Note that, in this case, these two hybrid systems have lost the advantage of the solar part as another alternative source to replace the wind in case of need. These topologies, despite the possibility of the battery power control, they will not benefit of the wind-sun compromise.

A novel integration of a PV-wind energy system with enhanced efficiency has been proposed in [6], (see Fig. 2 (d)).

This proposed system ensures the PV-grid integration by obviating the need of a conversion stage for PV power processing, and guaranteeing the PV MPPT function only by using the DC bus voltage control. This structure presents a great advantage with its lower number of power electronic converters. Despite its advantages, it loses some control freedom degrees of the solar part, where any large variation in solar weather conditions can lead to a large variation in the DC bus voltage especially in the PV MPPT mode. This can affect consequently the WECS optimal operation. In this condition, it will require disconnecting the PV part causing the loss of a significant amount of PV power.

The main aim of this work is the power quality and the capability enhancement of control and the management of a hybrid power system, consisting of a DFIG based WECS, a PVS and a BSU coupled under an efficient and compact integration (see Fig. 3) via a developed control and power management strategy. The outputs from the various generation sources of this hybrid system

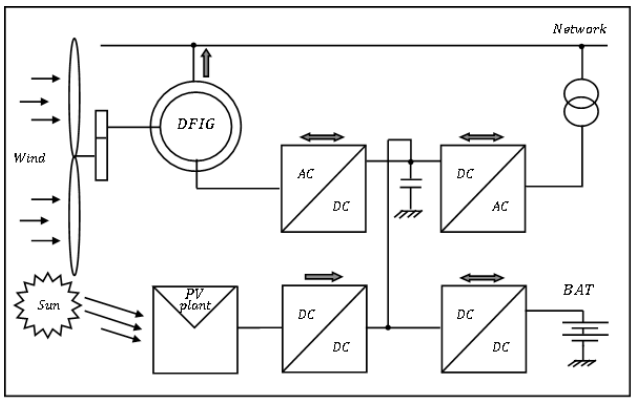

Fig. 3 Global description of the studied hybrid system

need to be coordinated and controlled for different operating modes (MPPT, a given power level and power generation quality enhancement). Thus, development of suitable power management that ensures sometimes meeting the network demand despite the intermittent nature of renewable sources is an integral part of ensuring the system reliability and achieving operational efficiency.

The proposed hybrid system associated with its control and power management strategy offers the following advantages:

1. Reduction of inverters number and their associated control circuits, therefore the overall cost of the system is reduced;
2. Optimal exploitation of the WECS Grid Side Converter (GSC) through which the PVS power flows in the proposed topology (especially around the WECS synchronous regime or for low wind speed operation);
3. Minimization of the grid-injected power fluctuation over a day;
4. Maintaining of the minimum energy production throughout the day and across the seasons (this is not the case for systems fed either only by solar PV source or only by wind turbine source);
5. Possibility of energy storage under batteries SOC control. Hence, the system performance increases;
6. Possibility of ensuring the MPPT mode operation;
7. Power quality enhancement with three different techniques.

2 Description of the studied system parts

This section presents a description of the studied hybrid system, consisting of a DFIG based WECS, a PVS and a BSU.

2.1 WECS description

The WECS is the main part of the presented hybrid system due to its greater power generation. The DFIG stator of this WECS is directly coupled to the grid line, while its rotor is coupled to the network through a back to back converter (see Fig. 4). This topology allows us to ensure the WECS control only by a third of its nominal power.

The studied WECS is based on a General Electric (GE) wind turbine with 1.5 MW of power [9]. Fig. 5 (a), (b) shows successively the produced total power and the rotor speed characteristics of this turbine versus the wind speed.

The wind ATLAS map of Algeria allows us to specify the average wind speed estimated at 10 m from the ground for different zones (see Fig. 6).

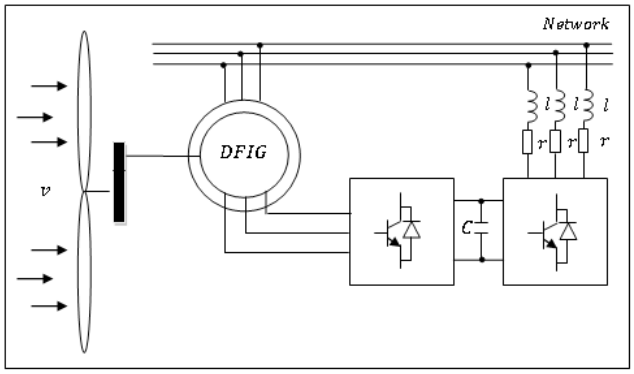

Fig. 4 Studied WECS description

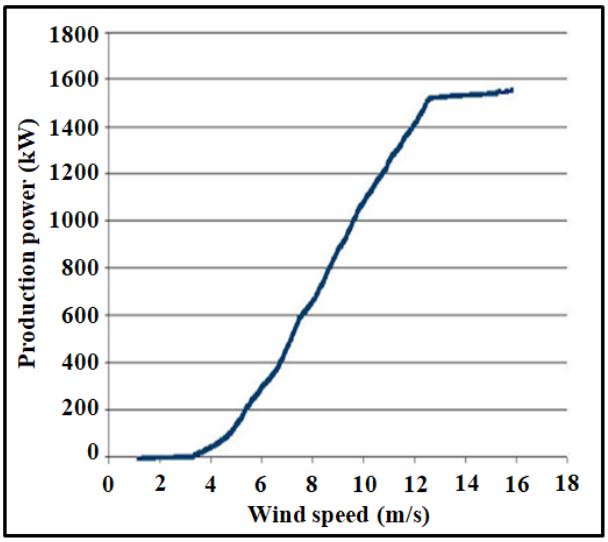

(a)

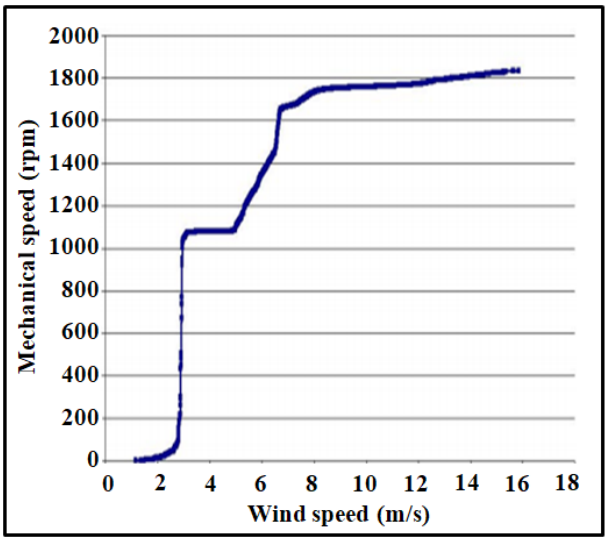

(b)

Fig. 5 (a) Real produced total power characteristic of the studied WECS (b) Real rotor speed characteristic of the studied WECS

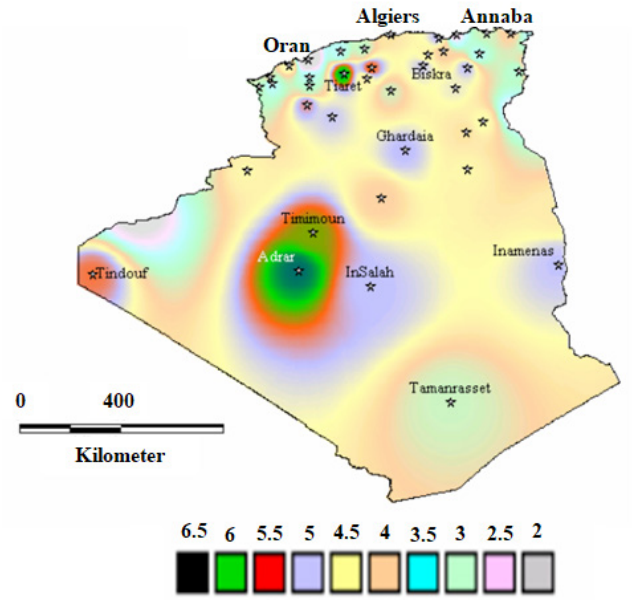

Fig. 6 ATLAS map of the annual mean wind speed in Algeria

It can be seen that Adrar site is the most windy site in Algeria. It presents a considerable wind field for the installation of wind turbine farms (10 MW wind farms actually installed in Kabertene site in Adrar).

The studied wind turbine of 1.5 MW must be installed at a height of 85 m (see the wind turbine characteristics in [9]). Therefore, it is initially important to estimate the wind speed for this altitude from the Adrar site available data for an altitude of 10 m. Using the Mikhail and Justus method, the vertical extrapolation of the wind speed distribution can be performed according to Table 1.

Fig. 7 shows the wind speed Weibull distribution for two heights 10 m and 85 m in the Adrar site.

Based on the wind turbine produced power characteristics shown in Fig. 5 (a) and the speed distribution presented in Table 1, the Swiss Wind Power Data Website (SWPDW) mandated by the Swiss Federal Office of Energy (SFOE) [10] has been used to plot on the same Fig. 8 (a), the wind speed distribution curve, the produced power curve and the power production distribution curve of the studied wind turbine using the meteorological data of Adrar site. Consequently, the power production during one year and the capacity factor of this wind turbine can be determined (see Table 2).

The capacity factor is the ratio between the annual production and the maximum technically possible production of a wind turbine. It should be noted that wind turbines are not principally designed for an optimal capacity factor, but to generate as much electricity as possible

Table 1 Vertical extrapolation of the wind speed distribution in Adrar site

Wind class (m/s)	Height of 10 (m)	Height of 85 (m)
	Weibull frequency in (%)	Weibull frequency in (%)
0.5	0.34	0.04
1.5	2.13	0.30
2.5	4.84	0.87
3.5	7.95	1.75
4.5	10.84	3.05
5.5	12.91	4.60
6.5	13.69	6.30
7.5	13.07	8.05
8.5	11.27	9.60
9.5	8.77	10.45
10.5	6.16	10.80
11.5	3.90	10.45
12.5	2.20	9.45
13.5	1.14	7.85
14.5	0.50	6.05
15.5	0.20	4.30
16.5	0.07	2.78
17.5	0.02	1.65
18.5	0.00	0.90
19.5	0.00	0.45
20.5	0.00	0.18
21.5	0.00	0.04
22.5	0.00	0.02
23.5	0.00	0.01
24.5	0.00	0.00
25.5	0.00	0.00
Mean wind speed (m/s) at 10 (m)	Weibull parameters at 10 (m)	
6.9	Scale factor (m/s)	Form factor
	7.8	2.68
Mean wind speed (m/s) at 85 (m)	Weibull parameters at 85 (m)	
10.5	Scale factor (m/s)	Form factor
	11.69	3.3

at certain wind speed. For this application, a value of 58.6 % is considered to be a very high capacity factor in terms of power wind exploitation.

In order to evaluate the capacity factor of the rotor back to back inverters, it is necessary to redo the application based on the Weibull calculator for the rotor as well. To achieve this calculation, the rotor power has to be known based on the WECS total power and the DFIG slip. This latter can be determined at each wind speed by using

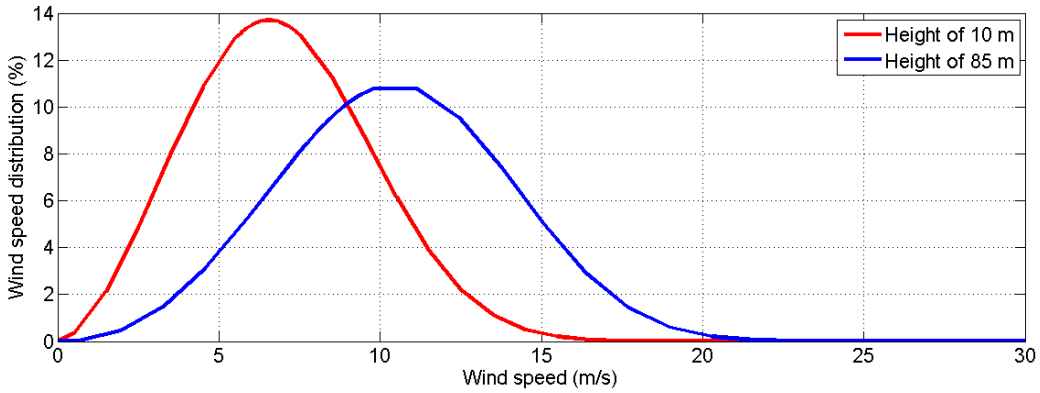

Fig. 7 Wind speed Weibull distribution in Adrar site for two different heights (10 m and 85 m)

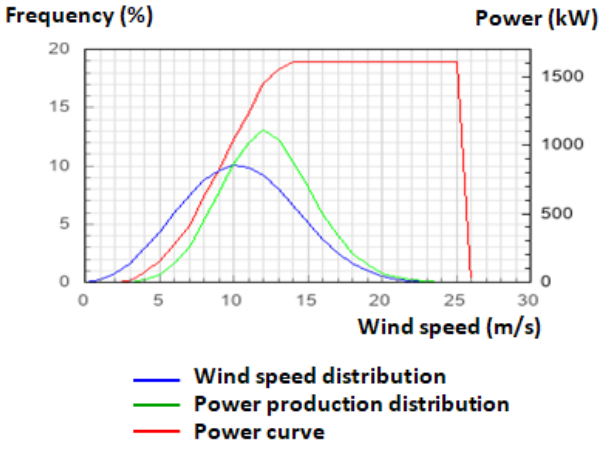

(a)

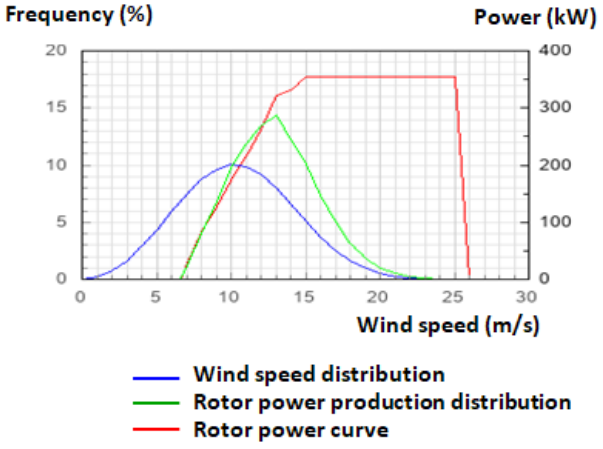

(b)

Fig. 8 (a) Total produced power characteristic of the GE 1.5 MW wind turbine evaluated at the region of Adrar (b) DFIG rotor power characteristic DFIG rotor power characteristic

Table 2 Weibull statistical analysis of the GE 1.5 MW wind turbine and estimation of its production at the region of Adrar

Characteristic of the total power delivered by the GE 1.5 MW wind turbine [9]			
Wind speed (m/s)	Total produced power (kW)	Wind speed (m/s)	Total produced power (kW)
1	0	16	1550
2	0	17	1550
3	5.7	18	1550
4	68.5	19	1550
5	150	20	1550
6	270	21	1550
7	400	22	1550
8	600	23	1550
9	800	24	1550
10	1000	25	1550
11	1200	26	0
12	1400	27	0
13	1500	28	0
14	1550	29	0
15	1550	30	0

Some statistical characteristics of the wind turbine studied on a site of Adrar	
Wind turbine capacity (kW)	1550
Power production (kWh/year)	8 926 736
Capacity factor (%)	65.7
Full load hours	5 755
Operating hours	8 674

the mechanical characteristic of the turbine (see Fig. 5 (b)). Table 3 presents the obtained results.

It is important to clarify that the power negative values presented in Table 3 concerning the rotor produced power means that the flow of power is being directed toward the rotor. As the wind speed exceeds the value of 6.8 m/s which is beyond the synchronism speed, this power changes to positive values which means that the rotor in operating on production mode.

Fig. 8 (b) shows, in the same time, the wind speed distribution curve, the rotor produced power curve and the rotor power production distribution curve. Based on Table 3, it can be concluded that the rotor capacity factor

Table 3 Weibull statistical analysis of the rotor production of the GE 1.5 MW wind turbine and estimation of this production at the Adrar site

Rotor power characteristic of the GE 1.5 MW wind turbine			
Wind speed (m/s)	Rotor produced power (kW)	Wind speed (m/s)	Rotor produced power (kW)
1	0	16	341
2	0	17	341
3	−4.385	18	341
4	−18.34	19	341
5	−39.73	20	341
6	−44.81	21	341
7	26.726	22	341
8	80.113	23	341
9	122.79	24	341
10	166.76	25	0
11	208	26	0
12	252	27	0
13	310	28	0
14	319.56	29	0
15	341	30	0

Some statistical characteristics of the rotor chain of the studied wind turbine	
Rotor capacity (kW)	341
Rotor total power (kWh/year)	1 568 130
Rotor produced power (without taking into account the negative part of the rotor power) (kWh/year)	1 613 359
Total capacity factor of the rotor (%)	52.5
Rotor capacity factor in production mode (%)	54.0
Full load hours (h/year)	4 595
Total operating hours (h/year)	8 674
Hours of operation in production mode (h/year)	7 376

is also good in terms of power wind exploitation (54 % in the production case).

However, an important remark arises concerning the back to back converter capacity factor level. To evaluate this latter, it is necessary to calculate the full annual energy of this converter that is designed to ensure a maximum power flow of 500 kW.

The annual full power flow of the back to back converter is calculated as follows:

$$E_{conv} = P_{conv} \times 24 \times 365 = 500 \times 24 \times 365 = 4\ 380\ 000\ \text{(kWh/year)}. \quad (1)$$

Then, the annual energy efficiency of this converter represents the electrical capacity factor which is the ratio between the rotor power production and the full power flow of the back to back converter (especially the GSC):

$$\eta_{conv} = E_{rot} / E_{conv} = 1\ 613\ 359 / 4\ 380\ 000 = 36.83\ (\%). \quad (2)$$

From the obtained results, it is clear that despite the good capacity factor of the WECS, the power electronics converter is not very well exploited (36.83 % as efficiency). But a better exploitation of such converter is an important and essential issue to be achieved. The integration of another source of energy to the rotor converter allows its better exploitation and improves the overall efficiency of the system. The hybridization of the WECS with a PVS connected to the DC bus presents a good solution for increasing the efficiency of the whole system and enriching the presented system by adding a complementary new renewable source to the existing wind source [6]. Theoretically, the PVS can contribute in increasing the converters capacity factor to exceed 60 % in the case of energy availability (Taking into account only the illuminated periods). In this paper, the presented hybrid system is studied on the basis of the Adrar site located in the south of Algeria, which is a rich sunlight area also (see Fig. 9). A 400 kW photovoltaic power plant can be installed to increase the GSC annual efficiency degree with more than 20 %. Taking into account the sunshine period of 6 hours per day at average conditions of 1000 W/m^2 as illumination and 25 °C as temperature, the new GSC annual energy efficiency can be recalculated as follows:

$$\eta_{GSC} = 36.83 + (400 \times 6 \times 365) / 4\ 380\ 000 = 56.83\ (\%). \quad (3)$$

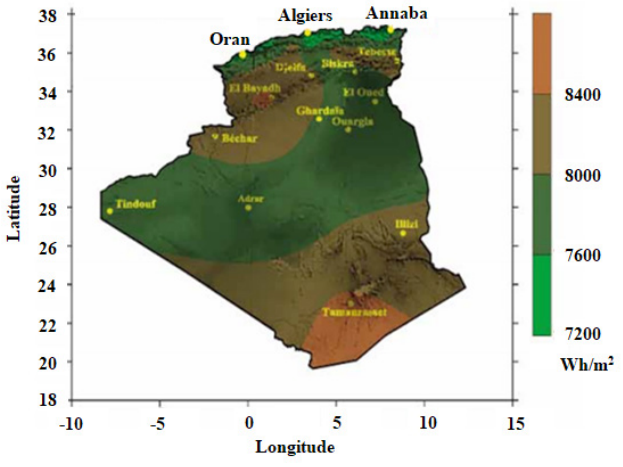

Fig. 9 ATLAS map of the annual mean of inclined total irradiation in Algeria

2.2 PVS description

Fig. 10 shows the description of the studied PVS. In order to respect the maximum power of the WECS converters, especially of the GSC, the PV plant is sized to provide a total power of 400 kW. Consequently, the photovoltaic field contains 2000 photovoltaic modules (BP SX 3200 type, with 200 Wp as power).

However, the output voltage of the PVS (600 V) needs to be boosted to reach 2000 V (DC bus voltage). Indeed, to achieve the PVS output voltage control, a boost converter is used to give a wide liberty degree for the proposed hybrid system. On the other side, the WECS inverters resizing will not be required as another merit of the use of the boost converter. The energy management algorithm proposed to pilot the whole proposed hybrid system power, prevents the GSC overrating. For this purpose, the boost converter can control and limit the PVS power, especially for the high wind speeds where the WECS production is high. As Wandhare and Agarwal [6] said, a GSC resizing approach has been proposed in order to support the eventual additional power, to ensure the PVS maximum production operation mode and to avoid the large variations of the DC bus voltage that can affect the WECS good operation.

2.3 BSU description

The BSU is designed to improve the performance of the hybrid system by increasing its energy efficiency. The excess energy will be stored in the batteries through a reversible buck-boost converter which allows to transfer the energy in both directions with the possibility of controlling the SOC of the batteries.

In case of meteorological fluctuations, the BSU plays a very important role in helping the system to ensure continuity of production at the limit of accumulated energy. In case of a strong wind and a high sunshine, the GSC will be exploited to the maximum and the surplus energy will be stored in the batteries with the possibility of limiting the WECS production or PVS production in case of maximum SOC. But, when the production of one renewable source is weak or vanishes (especially the PVS in the night), the batteries play a very important role for the compensation of the production lack in order to allow to the GSC to operate at a high level. It is possible to increase in some cases the GSC's performance more than 80 % by exploiting the three sources WECS, PVS and BSU at the same time.

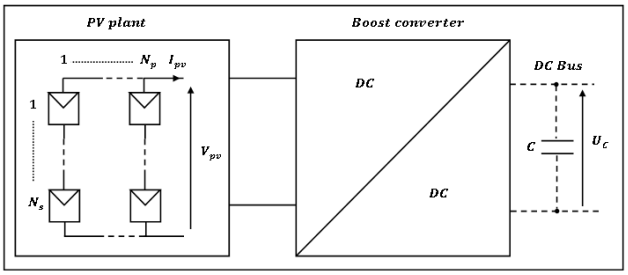

Fig. 10 PVS description

3 Modeling of the studied hybrid system

This section presents the modeling of the proposed hybrid power system presented previously in this paper (see Fig. 3).

3.1 WECS modeling

In order to establish the WECS model, the different components of this system will be modeled separately.

3.1.1 Aerodynamic power captured by the wind generator

According to Betz theorem and Newton's second law, the power extracted from the wind by a turbine is expressed in function of the wind speed v and the surface swept by the turbine blades S as shown in the following equation:

$$P_t = \frac{1}{2} C_p S v^3, \tag{4}$$

where:

- ρ is the air density and C_p is the turbine power coefficient which depends on the turbine specific speed λ and the blades pitch angle β.

Equation (5) represents the expression of the C_p for a wind turbine of 1.5 MW which is used in this study (these wind turbine parameters are summarized [9]:

$$C_p(\lambda,\beta) = \left(0.5 - 0.00167(\beta - 2)\right)\sin\left[\frac{\pi(\lambda + 0.1)}{\left(18.5 - 0.3(\beta - 2)\right)}\right] - 0.00184(\lambda - 3)(\beta - 2), \tag{5}$$

where the turbine specific speed is as follows:

$$\lambda = \frac{R\Omega_t}{v} \tag{6}$$

R is the blades radius; Ω_t is the rotation speed of the turbine and β is the pitch angle of the turbine blades.

3.1.2 Wind turbine modeling

It is supposed that the turbine has identical blades with very low friction coefficients and the wind speed has a uniform distribution over all the blades.

3.1.2.1 Wind speed modeling

The dynamic properties of the wind are very important for the study of a wind energy conversion system, because the wind power evolves in function of the cube of the wind speed cube, in the optimal conditions. The wind speed is a three dimensional vector. However, the direction of the wind considered velocity vector in this model is limited to the horizontal direction. The behavioral model of the wind speed can be simplified considerably. It is usually represented by a scalar function of time.

This function is decomposed into two components, a mean component which is varying very slowly, and a fluctuant term representing the sum of sine waveforms components. Hence the wind speed can be expressed as follows:

$$v(t) = v_0 + \sum_{i=1}^{n} A_i \sin\left(\omega_i t + \varphi_i\right), \tag{7}$$

where:

- v_0 is the average component;
- A_i, ω_i and φ_i are respectively, the amplitude, the angular frequency and the initial phase of each component of the fluctuant term.

Fig. 11 shows two different wind profiles, the first one reflects the stochasticity which can be found on a wind site and the second one is a filtered profile adapted to the studied aerogenerator in this paper, it presents a slow dynamic.

3.1.2.2 Turbine model

The aerodynamic torque can be determined based on the turbine rotation speed as follows:

$$T_{aer} = \frac{P_t}{\Omega_t} = \frac{1}{2\Omega_t} C_p \rho S v^3. \tag{8}$$

3.1.2.3 Dynamic equation of the generator shaft

By transforming of the turbine mechanical parameters to the generator shaft, the mechanical model is defined as follows:

$$J\frac{d\Omega_e}{dt} + D\Omega_e = T_g - T_{em} \tag{9}$$

with

$$J = J_t / G^2 + J_e \tag{10}$$

$$D = D_t / G^2 + D_e, \tag{11}$$

where:

- J_t, D_t, J_e, D_e, J and D are respectively, the inertia and the friction coefficient of the turbine, the generator and those brought on the generator shaft;
- G is the gain of the multiplier and T_g is the effect of the torque of the turbine on the generator shaft.

3.1.3 Relationship between DFIG stator powers and rotor currents

The two-phase reference (*d*-*q*) frame which is associated to the stator rotating field is used in this paper. The active and reactive powers of the DFIG stator can be obtained based on the Park transformation of the DFIG equations and the stator flux orientation on the *d* axis. In addition to the active and reactive power relations of the DFIG rotor, Eq. (12) presents the expressions of the active and reactive powers based on simplification hypothesis due to the high power rate of the studied wind turbine where the stator resistors are neglected [11].

$$\begin{cases} P_r = \dfrac{3}{2}\left(v_{dr} i_{dr} + v_{qr} i_{qr}\right) \\ Q_r = \dfrac{3}{2}\left(v_{qr} i_{dr} - v_{dr} i_{qr}\right) \\ P_s = -\dfrac{3}{2} v_s \dfrac{M}{L_s} i_{qr} \\ Q_s = \dfrac{3}{2}\left(\dfrac{v_s^{\,2}}{L_s \omega_s} - \dfrac{M}{L_s} v_s i_{dr}\right) \end{cases} \tag{12}$$

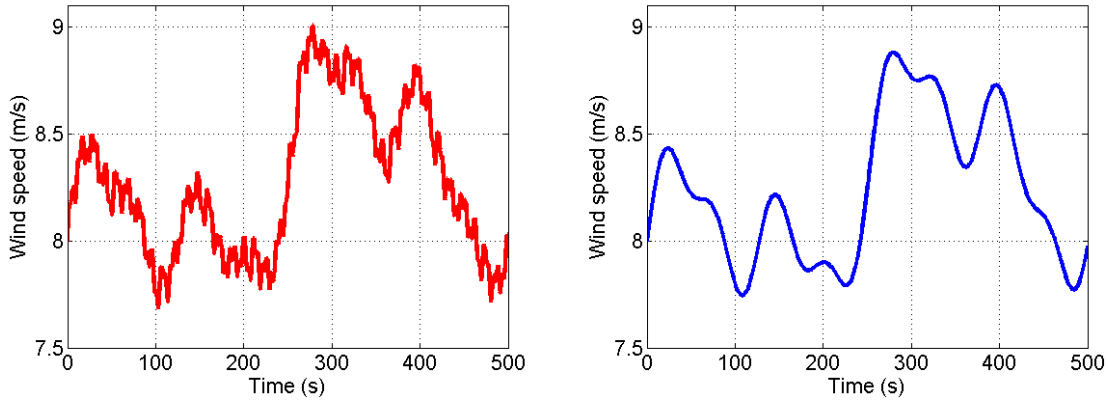

Fig. 11 Different wind profiles (Real and filtered)

From these last equations, it is apparent that the control of the stator active power and reactive powers are decoupled. Indeed, with a constant magnetizing inductance and a powerful network, the power P_s will be directly proportional to the current I_{qr}, and the power Q_s will be proportional to the current I_{dr} only, as shown in Eq. (12).

3.2 PVS modeling

Fig. 12 presents the PVS detailed description.

3.2.1 Modeling of the PV generator

The mathematical modeling of the PV cell is based on one exponential and four parameters (L4P) model, which is widely used in the literature. It treats the photovoltaic cell as a dependent current source of illumination which is connected in parallel with a diode and a resistance and in series with a resistance R_{ser} (see Fig. 12).

By neglecting of I_{sh} which is relatively very weak, the current given by this cell is expressed as follows:

$$I_{pv} = I_{ph} - I_s\left(e^{\left((V_{pv}+I_{pv}R_{ser})/(V_t n)\right)} - 1\right), \tag{13}$$

where:

- n is an ideality factor $(1 \le n \le 5)$;
- $V_t = \left((KT)/q\right)$ is the thermodynamic potential;
- T is the actual temperature of the cell in Kelvin;
- $q = 1.602 \cdot 10^{-23}$ (C) is the electron charge constant;
- $K = 1.38 \cdot 10^{-23}$ (J/K) is the Boltzmann constant;
- I_{ph} is the photocurrent ($I_{ph} \approx I_{pvsc}$);
- I_s is the reverse saturation current of a diode, it is expressed as follows:

$$I_s = C_s T^3 e^{\left((-E_{gap}q)/(nTK)\right)}, \tag{14}$$

where:

- $E_{gap} = 1.03,\ 1.12,\ 1.5$ or 1.7 (eV) (depending on the material of the cell) is the gap energy;
- C_s is the reference saturation current expressed as follows:

$$C_s = I_{pvsc} \Big/ \left(e^{\left(V_{pv0}/(nV_t)\right)} - 1\right) \tag{15}$$

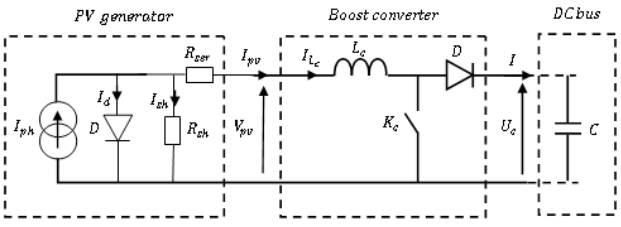

Fig. 12 PVS detailed description

whereas:

- I_{pvsc} is the short circuit current and V_{pv0} is the open circuit voltage of the cell.

To generalize the above equation to be valid for various meteorological conditions of temperature and illumination, the short circuit current and the open circuit voltage of the PV cell take their new expressions as follows:

$$\begin{cases} I_{pvsc} = \left(g/g_r\right)\left(I_{pvscref} + \mu_c\left(T - T_r\right)\right) \\ V_{pv0} = V_{pv0ref} - \mu_v\left(T - T_r\right) \end{cases}, \tag{16}$$

where:

- g and T are the actual illumination and temperature;
- $\mu_c, \mu_v, I_{pvscref}, V_{pv0ref}, g_r$ and T_r are respectively, the temperature influence factors on the short circuit current, the open circuit voltage, the reference of the short circuit current, the reference of the open circuit voltage, the illumination and the reference temperature. These parameters are given by the manufacturer.

3.2.2 Boost converter modeling

Fig. 12 presents the boost converter which is used to control the converted photovoltaic power. During the two complementary time intervals t_{on} and t_{off} in each period T_{conv}, the boost converter can be modeled as follows:

$$\begin{cases} di_{pv}/dt = \left(V_{pv} - (1-d)U_c\right)/L_c \\ du_c/dt = \left(I_{pv}(1-d) - I\right)/C \end{cases}. \tag{17}$$

3.3 Storage system modeling

To ensure a good power management between the two renewable sources (wind and solar) and the network, and to guarantee at the same time a smooth production of electrical energy, it is better to equip the proposed hybrid system with a battery unit. This device will ensure the energy storage when there is an extra production, or it acts as an extra source of generating, when there is an energy production deficiency of the other renewable energy sources. This unit is composed of a set of batteries coupled in series-parallel and connected to the DC bus of the hybrid system, via a bi-directional buck-boost converter (see Fig. 13).

As a part of maintaining the operation of the storage unit within the eligible limits, the voltage which is depending on the battery SOC needs to be controlled continuously. The SOC itself depends on the maximum capacity of battery $C_{\max}$, the current flowing in both cases of charging

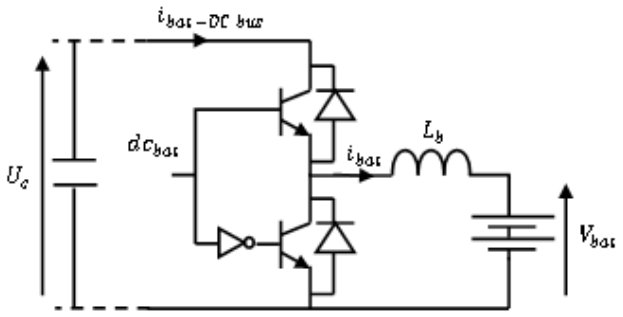

Fig. 13 Scheme of the storage system

and discharging i_{bat}, and the operating time, according to the following equation [12]:

$$\mathrm{SOC}(t+\Delta t) = \mathrm{SOC}(t) + i_{bat} \cdot \Delta t / C_{\max}. \quad (18)$$

This control allows to supervise the operation of the storage unit in the two modes. In the normal mode, when the batteries are connected to the hybrid system to assist the storage of the extra energy, or, to deliver a part of the electrical energy need in case of energy production deficiency of the other sources. The batteries are turned off, if they exceed their normal operating limits in terms of SOC and voltage.

4 Control of the hybrid studied system

This operation is done at any time by comparing the network requirement in terms of energy with the powers produced by the three components of the HS. In our case, the WECS always works in MPPT mode because of its slow dynamics. On other hand, the two elements (PVS and BSU) play their role in increasing production once or improving energy quality once again. Thus, their reference values in terms of energy to be produced are deduced from the difference between the network requirement and the power produced by the WECS.

To insure the hybrid system power management, it is necessary to pass through a low level control based on the control of each part individually before moving to the energy overall management.

4.1 WECS control

The WECS control is ensured by piloting the back to back converter composed of the RSC and the GSC.

4.1.1 Rotor side converter control

The RSC guarantee a decoupling active and reactive powers control of the DFIG (see Fig 14). This technique consists in synthesizing the control algorithm, from the investment

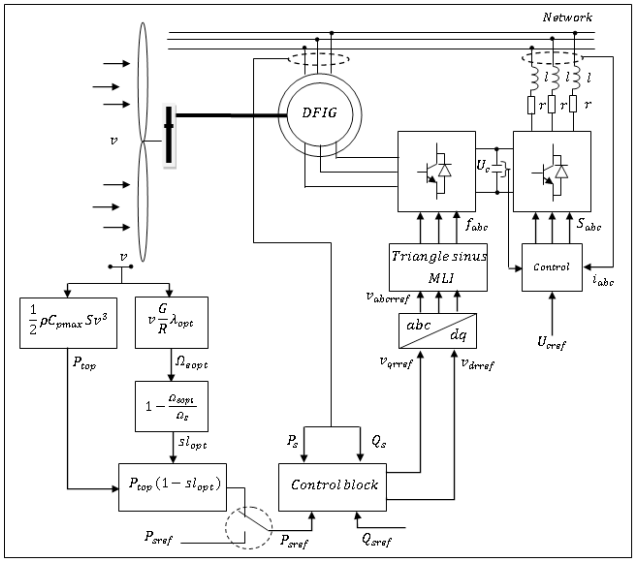

Fig. 14 Control scheme of the WECS back to back converter

of the mathematical model of the DFIG to develop the rotor reference voltages based on the references of the stator powers through two control loops, one for the stator powers and one for the rotor currents (see Fig. 15).

4.1.2 Grid side converter control

The GSC and its control block diagram are shown in Fig. 16. This control ensures the DC bus voltage U_c stabilisation and a unit power factor in the grid side.

4.2 PVS control

The PVS control based on PI controllers ensures the photovoltaic current, voltage and power control (see Fig. 17). Two control strategies have been performed, the first allows the production of a given requested power level in the limits of available weather conditions, and the second permits to achieve the MPPT mode.

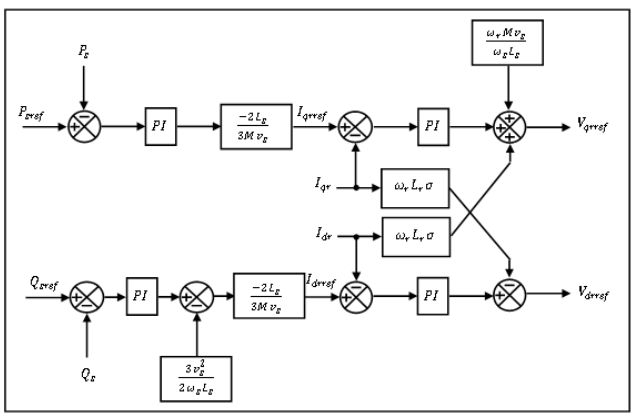

Fig. 15 Control loops of the DFIG stator powers

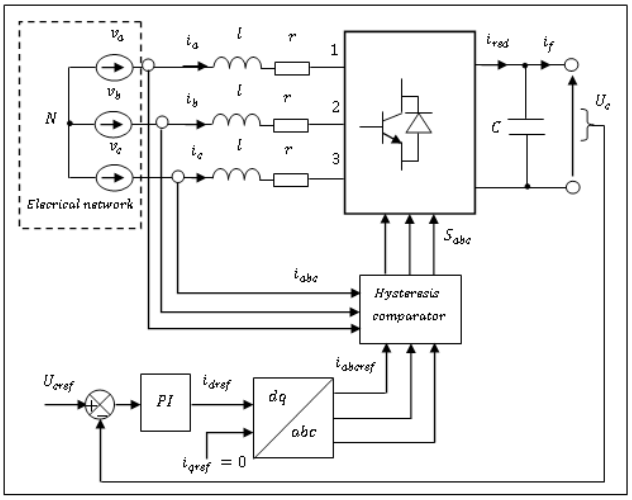

Fig. 16 Control scheme of the GSC

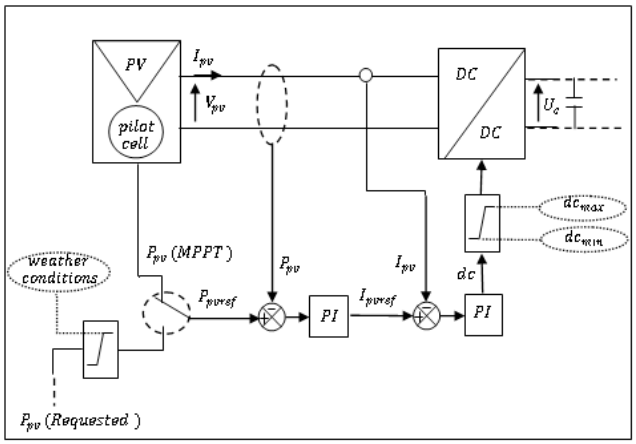

Fig. 17 Scheme of the PVS control loop

4.3 BSU control

The BSU control is made through the command of its bi-directional Buck-Boost converter by using a PI controller, as shown in the control loop of Fig. 18.

It can be seen in the last figure that the batteries command is based on the comparison between the desired total power and the powers produced by the WECS (P_{DFIG}) and the PVS.

This comparison allows obtaining the desired power of the BSU (in charge or discharge modes), from where it can possible to know the desired battery current (i_{batref}) by unscrewing the desired power value on the batteries

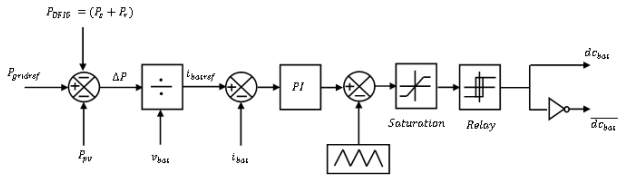

Fig. 18 Control loop of the storage system

voltage. The PI controller used allows controlling the difference between the reference value of the BSU current and the measured value to produce a voltage that will be compared with a triangular signal in order to deduce a logical control signal of the transistors of the BSU converter (Fig. 13).

5 MPPT and power quality enhancement of the hybrid power system

The studied hybrid system is supervised according to two levels, a central high level for power flow management between different sources and a local low level to control each source with its specific regulation loops. The proposed control strategy has been performed to ensure the energy management in two modes. The first, aims to ensure the MPPT for all sources (WECS and PVS without use of the BSU). The second mode aims to enhance the HS power quality by reducing the fluctuations of the output power for different weather conditions. This objective aims to smooth the total power produced by the hybrid system in a way that is different from unlike other works which deal the subject of energy quality for the hybrid systems through other techniques and according to other concepts, such as: the technique that applies the improved control strategy for power quality enhancement in standalone systems based on four-leg voltage source inverters (presented in [13]), the technique that aims to achieve the power quality improvement of single phase weak grid interfaced hybrid solar PV and wind system using double fundamental signal extracter-based control (presented in [14]), the technique aims to improve the voltage of remote connection using wind-solar farms equipped with new voltage control strategy based on virtual impedance monitoring (presented in [15]) and the technique which aims to improve the energy quality using a shunt active power filter (presented in [16]).

For our case, the second considered strategy, offers the possibility of power smoothing according to three techniques in order to meet the energy quality enhancement need. More accurately, the first technique aims to produce the desired network power by controlling the WECS to operate in its MPPT mode and piloting the PVS to ensure the total power smoothing. This technique, although it plays an important role in energy quality enhancement, it has a major drawback of losing much of photovoltaic power. Consequently, it is under exploited; especially in the case of wind high speed where the WECS mean production exceed the requested power level. To solve this problem, a second technique is proposed to smooth the total

produced power, on the basis of the average power values of the WECS and the PVS corresponding to the meteorological conditions (Solar illumination and wind speed). In this case, the WECS operates at its MPPT mode and the PVS is controlled in such a way to ensure a maximum of power (depending on weather conditions) and guarantee a smoothing of the WECS production power.

A third, advantageous and effective technique in terms of power production quantity and quality mode is proposed. That is to make operating the two sources WECS and PVS at their MPPT mode, while improving energy quality through a battery unit, that stores the energy excess or recover the already stored energy. In this technique, the battery charge level (SOC) is controlled in the range of the eligible threshold; otherwise, the produced power level by the two sources (WECS/PVS) will be decreased.

The proposed hybrid WEC-PV-BSU system and its control loops have been implemented under MATLAB software to verify the interest of the proposed hybridization topology to improve the exploitation degree of the available converters. Moreover, to verify also, the effectiveness of the proposed control strategy (especially the modified MPPT mode as a novel strategy of power management) in terms of the produced power quantity and quality. In this section, the obtained simulation results are presented and discussed.

5.1 Simulation results and discussion, MPPT mode case

In this case, the hybrid studied system devoid of BSU, is coupled to the grid. The PVS controlled to operate at its optimal point corresponding to the meteorological conditions. On the other side, the wind turbine is run to its optimal point, so that the wind turbine extracts the maximum possible power from the wind. The weather conditions considered (wind speed, temperature and irradiance) vary successively according to Fig. 11 (filtered profile) and Fig. 19 profiles respectively. Fig. 20 shows the simulation results for this case.

It is important to note that in all presented simulation stages, the powers generated by the components of the hybrid system take the negative values, while the absorbed powers will take positive values. This values sign are according to the DFIG modeling, which is based on the motor notion where the torque applied to the motor is inversed to ensure the generator operation mode. For the other components of the hybrid system such as PVS and batteries, the references of the produced powers are also taken negative to avoid the conflict with the DFIG produced power.

In the first simulation case, it can be seen that the simulation results confirms the efficiency of the MPPT controllers as the output powers perfectly follows their commands in the two sides, WECS and PVS. Obviously, the total produced power by the hybrid system is the sum of the power generated by the stator and the rotor of the DFIG and the PVS produced power. By a simple calculation of the GSC capacity factor based on the report between the Grid-GSC bond mean power and the GSC maximum power (500 kW) in each case (The mean value of the active power injected to the network on the side of the GSC divided by 500), it can be noted that it is improved from 19.5 % in the absence of the PVS, to 94.75 % in the case of the proposed hybrid system (WECS plus PVS).

$$\eta_{GSC} = \eta_{WECS\text{-}Rotor} + \eta_{PVS} = 19.5 + 75.25 = 94.75 \ (\%) \qquad (19)$$

It can be noted that, despite the good performance of the MPPT mode in terms of energy extraction quantity and capacity factor amelioration, the produced power is unfortunately fluctuant.

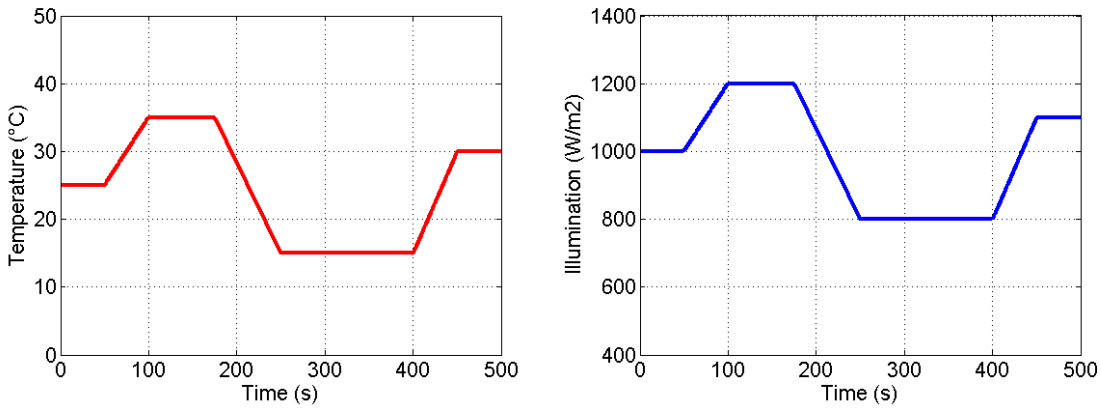

Fig. 19 Temperature and illumination profiles applied to the PVS

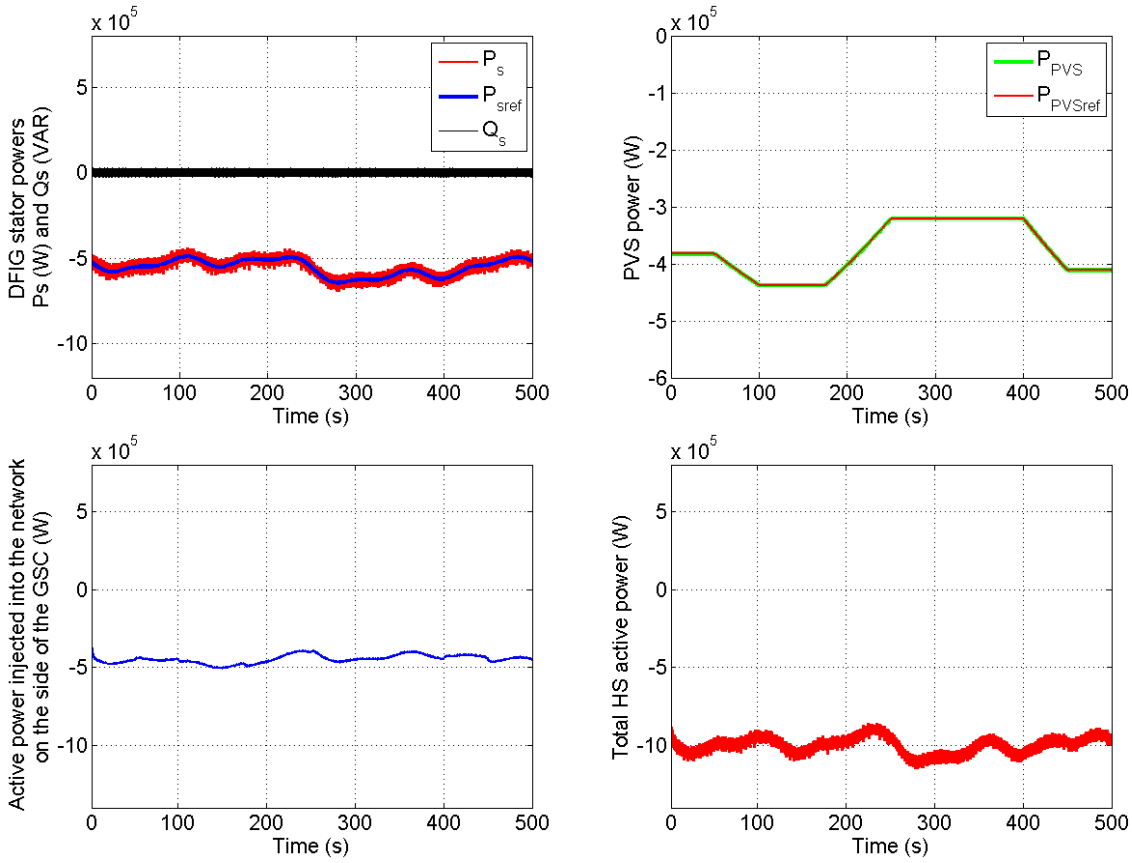

Fig. 20 MPPT mode results of the WEC-PV hybrid system

5.2 Simulation results and discussion, case of the Power Quality Enhancement Mode

In this second mode, various simulation results are obtained by proposing three smoothing control methods.

5.2.1 Power quality improvement via the PVS control

For the same previous weather conditions, the desired active power at the output of the HS is varying (650 kW in the beginning then 900 kW after 250 s) as shown in Fig. 21.

According to the obtained results, it can be noticed that the hybrid system produces the desired power which is the sum of the two source powers. In this case, the WECS operates at its MPPT mode and the PVS is used only to smooth the total HS delivered power, of course according to the weather conditions. Despite the effectiveness of this primitive technique in improving the power quality, it reduces the overall system performance since the PVS power is not well exploited. In fact, the injected power in the grid is covered in this case only by the WECS but the PVS produced power is considered to be a support to achieve the requested power level and eliminate the WECS power fluctuations. The capacity factor of the GSC in this case can be calculated also as follows:

$$\eta_{GSC} = \eta_{WECS\text{-}Rotor} + \eta_{PVS} = 19.5 + 30.65 = 50.15 \ (\%). \quad (20)$$

5.2.2 Modified MPPT mode for power quality enhancement

To improve the performance of the HS, it is proposed to exploit a maximum of the PVS power, while, at the same time, ensuring a smooth power at the output of the HS. Fig. 22 shows the simulation results of a modified MPPT technique which ensures a good compromise between the quantity and the quality of the total hybrid system produced power. Since, changes of temperature and illumination are slow comparatively to the wind speed fluctuation, it is assumed in this case that the temperature and the illumination are constants ($T = 25$ °C and $g = 1000$ W/m^2). The PVS power command is divided into two parts, a constant average part and a fluctuating part which is used to compensate the rapid changes in the available power of the WECS, which is still operating in the MPPT mode. It can be noted that this technique ensures a smooth of the HS total delivered power. From the obtained results, it can be noticed also that for some periods, the PVS production is limited by the weather conditions and it is not able to smooth the HS total delivered power. Moreover, during the other periods, the PVS injects a maximum of power while at the same time, contributes successfully to improve the power quality injected in the grid.

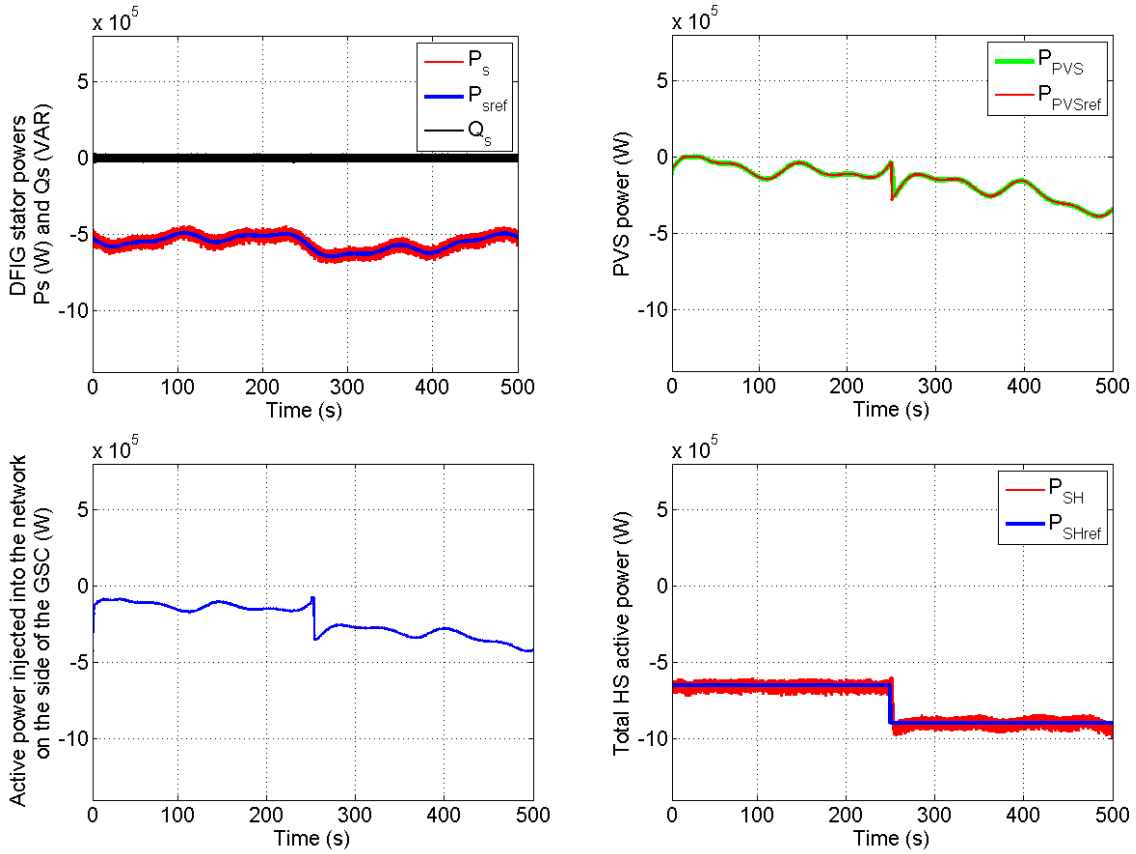

Fig. 21 Simulation results of the HS controlled to produce different smooth power levels

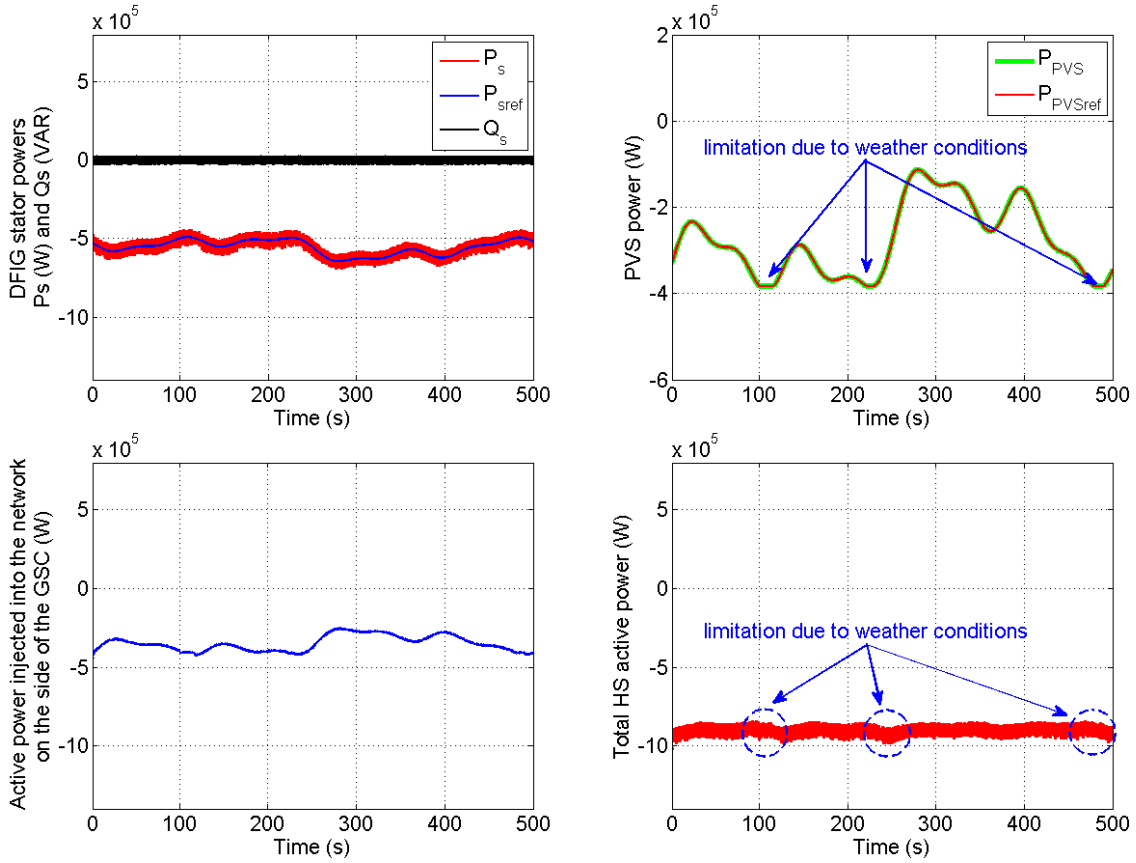

Fig. 22 Modified MPPT mode results

Similarly, the capacity factor of the GSC can be calculated as shown in Eq. (21):

$$\eta_{\text{GSC}} = \eta_{\text{WECS-Rotor}} + \eta_{\text{PVS}} = 19.5 + 55.5 = 75 \ (\%). \tag{21}$$

Note that this factor has been improved from 19.5 % in the case of PVS absence to 75 % in the case of the last proposed technique.

5.2.3 Power quality enhancement of the hybrid system using the BSU

In this case, the hybrid proposed WEC-PV system is equipped by a BSU, which produces or consumes the transient power below or above the grid requested energy (800 kW in this application). The control strategy in this case, has been successfully applied to manage the BSU power, for charging batteries with the surplus power, while at the same time controlling their SOC. The simulation results have been plotted in Fig. 23. It is clear seen in this figure, that the proposed smoothing control method can supervise the SOC to secure the charging level of the BSU by PVS production limitation (after 400 s), in case of BSU fully charged (100 % SOC). This technique, with properly allocating total power demand between the hybrid system sources, can ensure also the limitation of WECS production in necessary case. It is the case of wind high speed level where it is obligatory to not exceed the nominal power of the grid side converter (500 kW, one third from the nominal power of DFIG), which is not oversized.

Let us calculate once more the global capacity factor of the GSC:

$$\begin{aligned}\eta_{\text{GSC}} &= \left(\eta_{\text{WECS-Rotor}} + \eta_{\text{PVS}} + \eta_{Bat_{\text{discharge}}}\right) - \eta_{Bat_{\text{charge}}} \\ &= \left(19.5 + 68.17 + 0\right) - 33.18 = 54.49 \ (\%).\end{aligned} \tag{22}$$

Note that the GSC exploitation is more exploited to reach 54.49 % in the case of the WEC-PV-BSU hybrid system.

6 Conclusion

In this paper, a special coupling of various sources (WECS, PVS and BSU) of a hybrid system has been proposed. It allowed us to increase the operating capacity factor of the WECS rotor non resized converters (especially the GSC) more of 50 %. Moreover, this paper discussed a control and management strategy of the energy given by the system based on the energy availability and network need. The studied HS has been tested by simulation to evaluate the effectiveness of this power management strategy in two modes. The first is the MPPT mode, where the simulation results illustrate the effectiveness of the control strategy to extract optimum energy from the two sources (WECS and PVS). In the second mode, a power quality enhancement is observed at the hybrid system output, compared to the first mode. This has been achieved by three techniques, power smoothing only using a small part of the PVS power, power smoothing with the modified MPPT mode applied at the PVS as a novel proposed technique to achieve a good compromise between the quantity and the quality of power and power smoothing with BSU. In this latter case, a realistic control of battery state of charge (SOC) is ensured via the limitation of the PVS produced power in case of battery fully charging (100 % SOC). It has been noted also that the proposed control strategy is capable of getting both the MPPT, the power smoothing, the SOC control. Furthermore, this study presents the implementation possibility of the studied WECS and PVS in Adrar site which presents the windiest zone in the south of Algeria.

Appendix

Features of the used WECS [9]:

- Wind turbine parameters: R = 35.25 m; G = 90; λ_{op} = 9; $C_{p\max}$ = 0.9.
- Generator parameters: R_s = 0.012 Ω; R_r = 0.021 Ω; M = 0.0135 H; L_s = 0.0137 H; L_r = 0.0136 H; J = 1000 kg/m^3; D = 0.0024 N·m·s/rd; p = 2.
- DC bus and rotor-side filter parameters: U_c = 2000 V; C = 4400 µF; r = 0.002e^{-3} Ω; l = 5e^{-3} H.
- Parameters of used PV panels (BP SX 3200 Model): $P_{\max}$ = 200 Wc; V_{pvopt} = 24.5 V; I_{pvopt} = 8.6 A; I_{pvsc} = 8.7 A; V_{pv0} = 30.8 V.
- BSU parameters: V_{bat} = 12 V; $C_{\max/bat}$ =100 Ah; $L_{\text{BSUconverter}}$ = 1e-3 H; V_{BSUmin} =498.96 V; V_{BSUmax} = 604.8 V; $\text{SOC}_{\min}$ = 30 %; $\text{SOC}_{\max}$ = 100 %.

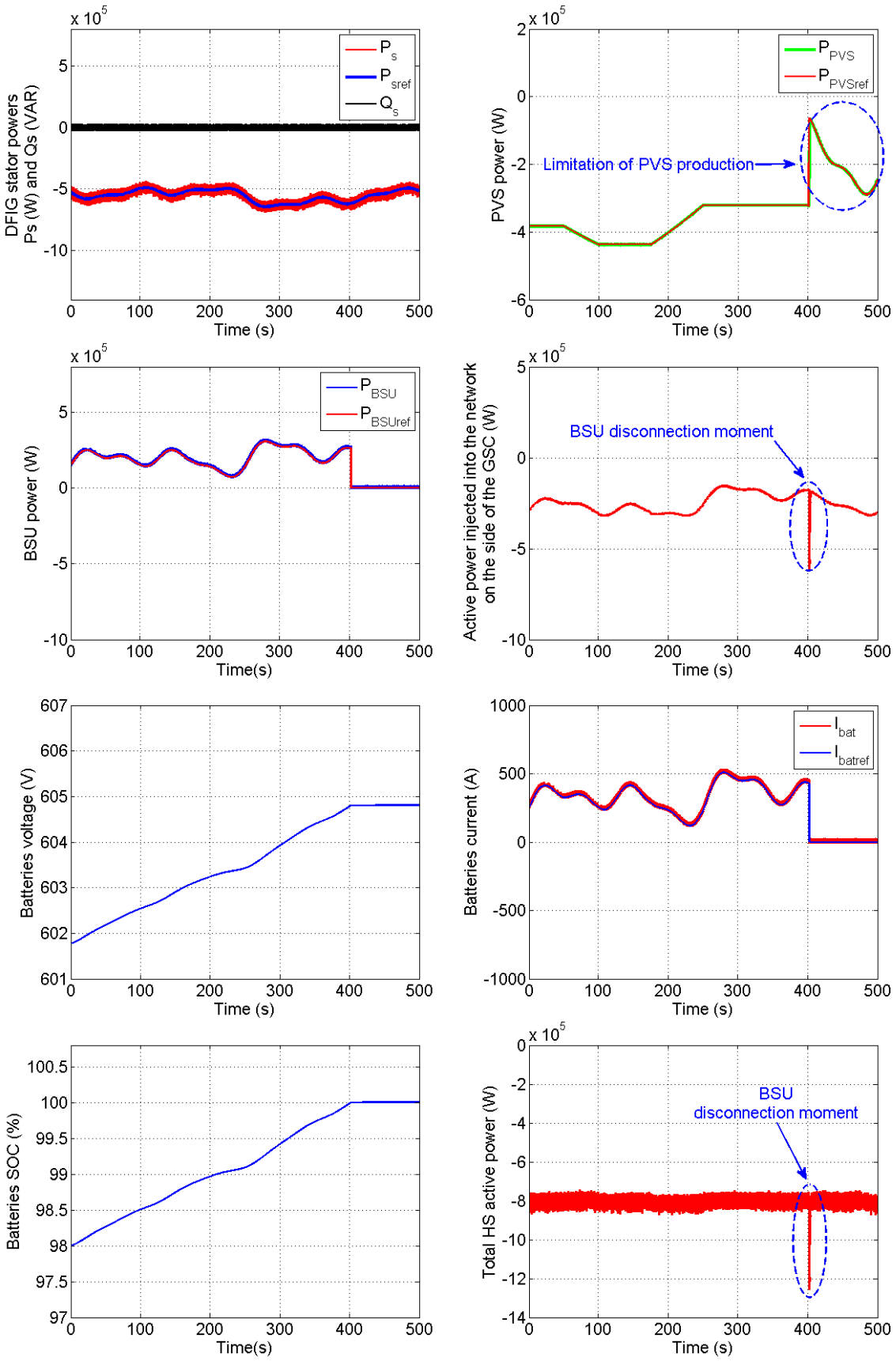

Fig. 23 Simulation results of the whole WEC-PV-BSU hybrid system

References

[1] U.S. Energy Information Administration (EIA) "Annual Energy Outlook 2015: with projections to 2040", U.S. Energy Information Administration, Office of Integrated and International Energy Analysis, U.S. Department of Energy, Washington, DC, USA, Rep. DOE/EIA-0383(2015), 2015. [online] Available at: https://www.eia.gov/outlooks/aeo/pdf/0383(2015).pdf [Accessed: 17 January 2018]

[2] Trifkovic, M., Sheikhzadeh, M., Nigim, K., Daoutidis, P. "Modeling and Control of a Renewable Hybrid Energy System with Hydrogen Storage", IEEE Transactions on Control Systems Technology, 22(1), pp. 169–179, 2014. https://doi.org/10.1109/TCST.2013.2248156

[3] Alnejaili, T., Drid, S., Mehdi, D., Chrifi-Alaoui, L., Belarbi, R., Hamdouni, A. "Dynamic control and advanced load management of a stand-alone hybrid renewable power system for remote housing", Energy Conversion and Management, 105, pp. 377–392, 2015. https://doi.org/10.1016/j.enconman.2015.07.080

[4] Kahla, S., Soufi, Y., Sedraoui, M., Bechouat, M. "On-Off control based particle swarm optimization for maximum power point tracking of wind turbine equipped by DFIG connected to the grid with energy storage", International Journal of Hydrogen Energy, 40(39), pp. 13749–13758, 2015. https://doi.org/10.1016/j.ijhydene.2015.05.007

[5] Munteanu, I., Bratcu, A. I., Cutululis, N. A., Ceangă, E. "Optimal Control of Wind Energy Systems: Towards a Global Approach", Springer-Verlag, London, UK, 2008. https://www.doi.org/10.1007/978-1-84800-080-3

[6] Wandhare, R. G., Agarwal, V. "Novel Integration of a PV-Wind Energy System With Enhanced Efficiency", IEEE Transactions on Power Electronics, 30(7), pp. 3638–3649, 2015. https://doi.org/10.1109/TPEL.2014.2345766

[7] Ghoddami, H., Delghavi, M. B., Yazdani, A. "An integrated wind-photovoltaic-battery system with reduced power-electronic interface and fast control for grid-tied and off-grid applications", Renewable Energy, 45, pp. 128–137, 2012. https://doi.org/10.1016/j.renene.2012.02.016

[8] Mendis, N., Muttaqi, K. "An integrated control approach for stand-alone operation of a hybridised wind turbine generating system with maximum power extraction capability", International Journal of Electrical Power & Energy Systems, 49, pp. 339–348, 2013. https://doi.org/10.1016/j.ijepes.2013.01.020

[9] El Aimani, S. "Modelisation de Differentes Technologies D'eoliennes Integrees dans un Reseau de Moyenne Tension" (Modeling of Different Wind Turbine Technologies Integrated in a Medium Voltage Network), PhD Thesis, University of Lille, 2004. [online] Available at: http://l2ep.univ-lille1.fr/fileupload/file/theses/SalmaElAimani.pdf [Accessed: 19 April 2018] (in French)

[10] Suisse Eole "The Swiss Wind Power Data Website", [online] Available at: https://wind-data.ch/index.php?lng=en [Accessed: 12 February 2018]

[11] Boutoubat, M., Mokrani, L., Machmoum, M. "Control of a wind energy conversion system equipped by a DFIG for active power generation and power quality improvement", Renewable Energy, 50, pp. 378–386, 2013. https://doi.org/10.1016/j.renene.2012.06.058

[12] Bouabdallah, A., Olivier, J. C., Bourguet, S., Machmoum, M., Schaeffer, E. "Safe sizing methodology applied to a standalone photovoltaic system", Renewable Energy, 80, pp. 266–274, 2015. https://doi.org/10.1016/j.renene.2015.02.007

[13] Houari, A., Djerioui, A., Saim, A., Ait-Ahmed, M., Machmoum, M. "Improved control strategy for power quality enhancement in standalone systems based on four-leg voltage source inverters", IET Power Electronics, 11(3), pp. 515–523, 2018. [online] Available at: https://digital-library.theiet.org/content/journals/10.1049/iet-pel.2017.0124 [Accessed: 23 September 2019]

[14] Gupta, T. N., Murshid, S., Singh, B. "Power quality improvement of single phase weak grid interfaced hybrid solar PV and wind system using double fundamental signal extracter-based control", IET Generation, Transmission & Distribution, 13(17), pp. 3988–3998, 2019. [online] Available at: https://digital-library.theiet.org/content/journals/10.1049/iet-gtd.2018.6647 [Accessed: 27 September 2019]

[15] Aghanoori, N., Masoum, M. A. S., Islam, S., Abu-Siada, A., Nethery, S. "Improving voltage of remote connection using wind-solar farms equipped with new voltage control strategy based on virtual impedance monitoring enabled by IEC 61850 communication", IET Generation, Transmission & Distribution, 13(11), pp. 2199–2207, 2019. [online] Available at: https://digital-library.theiet.org/content/journals/10.1049/iet-gtd.2018.5718 [Accessed: 03 October 2019]

[16] Chelli, Z., Lakehal, A., Khoualdia, T., Djeghader, Y. "Study on Shunt Active Power Filter Control Strategies of Three-phase Grid-connected Photovoltaic Systems", Periodica Polytechnica Electrical Engineering and Computer Science, 63(3), pp. 213–226, 2019. https://doi.org/10.3311/PPee.14025